Comparison of Different Methods for Extracting Bone Cross-Sectional Geometric Properties from CT Images

Siniša S. Ilić[1], Slađan Timotijević[2], Dejan Lazović[1], Petar Spalević[1], Alempije Veljović[3]

Abstract: Analysis of the geometric properties of bone cross-sections is often used to determine skeletal performance and the ability of the body to resist different external forces. This analysis is dependent on obtaining adequate bone cross-sectional images. CT images can be used for this purpose by performing some pre-processing of images in order to achieve sufficient accuracy. In this paper we have used experiments to show that relatively good accuracy of bone cross sectional areas and moments of inertia can be achieved by simple threshold level filtering of CT images.

Keywords: Image Processing, Edge detection, Bone Cross-Sections, CT Images.

1 Introduction

The cross-sectional geometric properties of bone shafts in long bones determine their behavior – their resistance to the external forces acting on them. It can be recognized by six basic kinds of strain: stretching, pressure, shearing, bending, torsion and buckling. In order to study all these properties, it is important to determine how cortical cross-section varies along the shaft axis of bone.

One of the ways to perceive how the bone cross-section is changing quantitatively was explained in [1]. Cadaver humerus was cut by Gili's saw into 18 pieces and the cross-section of each piece coloured by ink and paper prints created from them. These prints were enlarged and printed on graph paper with 1mm x 1mm matrix. The cross sectional area was determined by counting the "inked" squares.

The analysis of cross-sectional properties of bones is made easier through the use of Computed Tomography (CT). CT enables the acquisition of two-

---

[1]Faculty of Technical Sciences, University of Priština (at K. Mitrovica), Knjaza Miloša 7, 28220 Kosovska Mitrovica, Serbia;   E-mails: sinisa.ilic@pr.ac.rs, dejan.lazovic@pr.ac.rs , petar.spalevic@pr.ac.rs
[2]Clinical and Hospital centre "Bežanijska kosa", Bežanijska kosa b.b., 11080 Belgrade, Serbia;
  E-mail: sladjant@open.telekom.rs
[3]Faculty of Technical Sciences Čačak, Svetog Save 65, 32000 Čačak, Serbia;   E-mail: alempije@beotel.net

dimensional X-ray images of thin "slices" through the body. Multiple images from adjacent slices can be obtained in order to reconstruct a three-dimensional volume [2]. As output, CT creates set of digital gray scale 2-D images where pixel values represent so called Hounsfield units. The Hounsfield unit (HU) scale is a linear transformation of the original linear attenuation coefficient measurement into one in which the radio-density of distilled water is defined as zero HU, while the radio-density of air is defined as −1000 HU. The typical values of some tissues are: blood 30 − 45, muscle 40, soft tissue 100 to 300, bone 700 (cancellous bone) to 3000 (dense bone) [3].

The cross-sectional geometrical properties of the sample bones (distal radius and ulna in large, medium and toy breed dogs) are analyzed using CT images in [4]. Radial and ulnar cross-sections are approximated by elliptical rings with or without eccentric empty holes representing the medullar cavity. The longer and shorter diameters of outer and inner ellipses are estimated and measured for each image "slice" manually.

Nowadays, Health Institutions can purchase software packages for the detailed analysis of CT images. Some of these offer simple tools for users to measure distances between selected pixels on CT image, angles between some lines etc., while more sophisticated tools can calculate the Mineral Bone Densities (MBD) using peripheral Quantitative Computed Tomography (pQCT). Quantitative computed tomography (QCT) is a medical technique that measures bone mineral density (BMD) using a standard X-ray CT scanner with a calibration standard to convert Hounsfield Units (HU) of the CT image to bone mineral density values.

However, any such analysis is still dependent on obtaining adequate bone cross-sectional images. In [5] a structural analysis was performed to calculate the resistance of the affected bones to compressive, bending, and torsional loads using CT images. Calculation of cross-sectional areas is done by obtaining values E_i, which represent the modulus of the ith pixel, which is a function of the bone density at that pixel. The structural rigidity of the entire cross section is calculated from CT images as the sum of the product of the modulus (E_i) and the differential area (da – pixel size of CT image), to give the weighted area (E_ida) for each pixel at the position (x_i, y_i) relative to the modulus weighted centroid.

Some other comparisons of cross-sectional properties of bones using pQCT images of normal people and athletes are also given in [6], tennis players in [7], and older people in [8]; and also in an evaluation of a 3D object registration method for analysis of humeral kinematics [9].

CT images of bones are also studied in order to create a semi-automatic segmentation method based on active contour [10], and a method for extracting

outer bone surfaces from a 3D CT and generate 3D mesh of the bone surface using the marching cubes algorithm [11].

1.1 Definition of the problem

The resolution of the CT image is sometimes insufficient to precisely delineate the bone's boundary. Typical values for pixels in CT images of cortical tissue (bone) are over 1000 HU (the dark squares in Fig. 1), whereas values of pixels not completely occupied by bone are lower (the paler squares in Fig. 1). This is because the attenuation coefficients of bones are significantly larger than those of muscles and other tissues around the bone; hence the "intensity" of image elements in the vicinity of bone is proportional to the cortical area that the pixel covers. Also, it must be considered that there are other tissues around the bone (such as muscle, marrowbone, etc.) for which HU values of pixels are less than 150, and others, such as bone septa, with values greater than 150 HU.

pixel with area ΔA
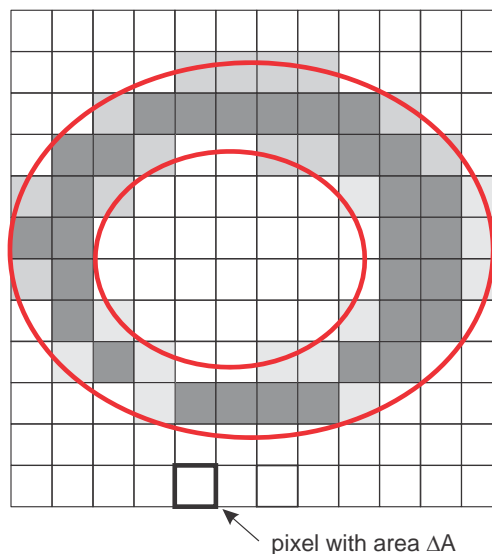
Fig. 1 – *Mapping of bone's attenuation coefficients into* HU *values in* CT *image pixels* (*pixels are presented as squares*).

If one wants to calculate the cortical area (the area occupied by bone) in a CT image, it seems that it can be obtained by counting the pixels that are occupied by bone (have large HU values) and multiply this count by the area of the pixel ΔA. As can be seen from Fig. 1, pixels with large HU values (the dark squares in Fig. 1) do not completely cover the bone area. It is obvious that the area obtained by selecting pixels with large HU values is less than total cortical area. It is necessary to first set a filter on pixel values – the pixels with values

greater than a defined threshold level will be counted and pixels with values less than the threshold will be ignored. The problem we investigated in this paper was the threshold level that should be implemented in such a filter in order to obtain as accurate an estimation of the cortical area as can be achieved.

2 Material

We used CT images of cross-sections of both, left and right, femurs (thigh bones) of a female person of older age obtained from the Clinical and Hospital Centre "Bežanijska kosa" in Belgrade. The CT device used was a Brilliance CT 64-channel scanner with a resolution of 512×512 pixels and 12 bit quantization (values from –1024 to 3071). The CT images were obtained by moving the patient by 1mm for each slice. The cross-sections obtained are from the distal line of trochanter minor to the base of the patella.

The CT study we performed was approved by the Institutional Ethical Committee of CH Center "Bežanijska kosa".

In our study DFOV (Display Field Of View) was 499 mm, the matrix size 512×512 and the real pixel size was 0.975mm×0.975mm. The tube voltage was 120 kV, the tube current was 136 mA and the slice thickness was 1 mm.

3 Methods

Due to our inability to obtain CT images of cross-sections of bone with higher resolution which would have been more adequate for our experiment, we determined the threshold level based on the bones' inner and outer contours obtained by Canny edge detection algorithm for images with four times higher resolution by using linear interpolation.

3.1 Preparation of the set of images

In order to obtain the cross sectional area of bone from the original resolution of the CT images, we performed the following sequence of steps:

1. Two rectangular frames were created, one for each bone (left and right femur), sufficient to contain all cross sections of bones in consecutive CT images along the length of the femur (see Fig. 2). It is possible for the cross section of bone to be in the top left part of the frame in the first slice and in the bottom right in the last;

2. Each CT "frame" image obtained in the previous step was resized by placing the cross section of bone in the centre of the frame. We "recognized" bone cross section by filtering pixel levels of CT image above 800 HU and left 4 to 8 pixels surrounding the bone contour we obtained (see Fig. 3a);

3. From the resized image, by implementing Canny edge detection method on bone, we obtained two contours – the inner and outer bone contour (see Fig. 3c).

We also performed the following steps in order to generate CT images with higher resolution:

4. From each resized image obtained in step 2, we created 3 new images by re-sampling (with factor 4) the original image using three interpolation methods – linear, cubic and cubic-spline - thus increasing the resolution of the image four times (see Fig. 3b, created using linear interpolation);

5. From the resized images with enhanced resolution (from the linear interpolation method), by implementing Canny edge detection of bones we again obtained two contours – inner and outer bone contour – with better resolution (see Fig. 3d).
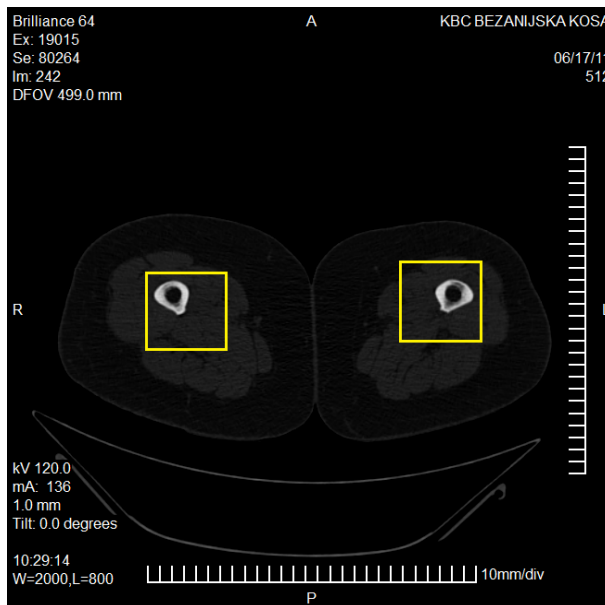

Fig. 2 – *Manual creation of two image frames for left and right femur in order to fit each* CT *image along the femur shaft.*

Images obtained in step 2 (with original resolution) were passed through the level filter by setting the threshold to 200, 300, 400, 500, 600 and 700 HU. We named this group of images Group **GFilt**$_{orig}$. Images obtained in step 4 (with enhanced resolution) were passed through the level filters using the same threshold levels and this group of images we named Group **GFilt**$_{high}$.

3.2 Analysis

We used the area between outer and inner contour obtained from the Canny edge detection in both the original and linear interpolated CT images (see figures 3c and 3d) as references **Ref**$_{orig}$ and **Ref**$_{high}$, and performed comparisons of the cortical areas of all images obtained in step 6 against these references. We also calculated the moment of inertia of the referenced area (from the image obtained in step 5 – **Ref**$_{high}$) and compared it with the calculated moment of inertia of bones detected in all other CT images (from the CT images obtained in steps 2 and 4).

The Canny edge detection algorithm that we used is performed in several steps [12, 13]. First of all, a 5×5 Gaussian filter is used to reduce the noise in the images (with $\sigma = 1$), then the typical Sobel Filter is used to calculate the initial edge strength distribution, and the Canny Edge Detection algorithm is used to extract the single-pixel-width edges based on the edge distribution obtained from the Sobel Filter. To improve the processing speed, a global strength threshold is introduced to eliminate the edge pixels with Sobel Gradient values under this threshold.

(a)　　　　　　　　　(b)

(d)　　　　　　　　　(e)
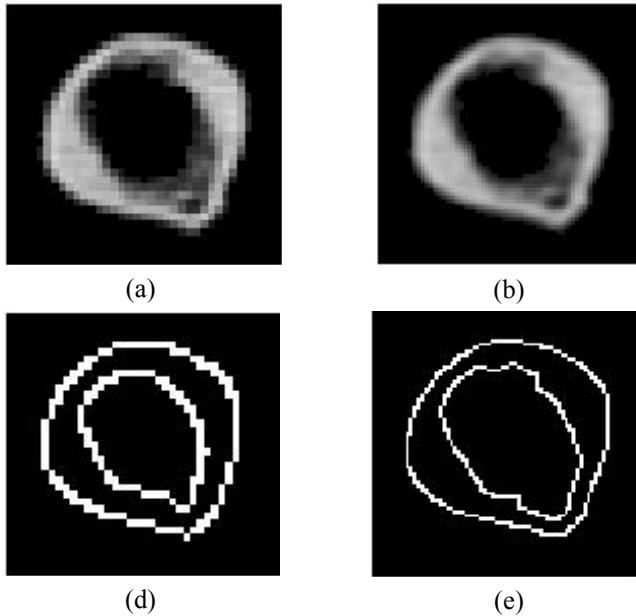
Fig. 3 – CT *images of femur*: (a*) in original scanned resolution,*
(b) *in four times higher resolution generated by linear interpolation,*
(c) *Canny edge detection from image* (a)*,*
(d) *Canny edge detection from image* (b).

(a)   (b)

(c)   (d)
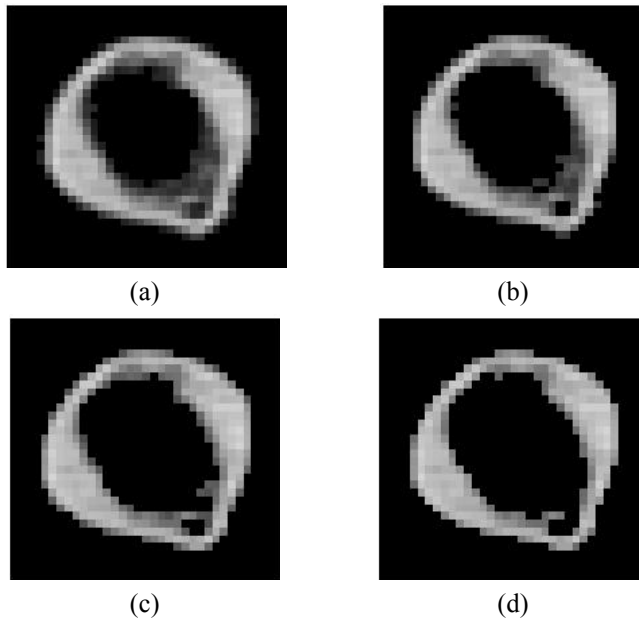
Fig. 4 – CT images of femur: (a) with levels greater than 200 HU,
(b) with levels greater than 400 HU; (c) with levels greater than 600 HU;
(d) with levels greater than 700 HU.

Fig. 5 – CT *images of femur after implementing
the Canny edge detection algorithm.*

As the expected outcome of the detection algorithm was two contours, we also implemented an algorithm for tracing contours, and thus we eliminated lines that didn't belong to the contours: Fig. 5 presents such a case.

The area moment of inertia was calculated using the following equations [14] for axial (1) and (2), centrifugal (3), polar (4) and principle moments of inertia (5) and (6):

$$I_x = \iint\limits_{(A)} y^2 \, \mathrm{d} A, \tag{1}$$

$$I_y = \iint\limits_{(A)} x^2 \, \mathrm{d} A, \tag{2}$$

$$I_{xy} = \iint\limits_{(A)} xy \, \mathrm{d} A, \tag{3}$$

$$I_0 = \iint\limits_{(A)} (x^2 + y^2) \, \mathrm{d} A = I_x + I_y, \tag{4}$$

$$I_1 = \frac{I_x + I_y}{2} + \frac{\sqrt{(I_x - I_y)^2 + 4I_{xy}^2}}{2}, \tag{5}$$

$$I_2 = \frac{I_x + I_y}{2} - \frac{\sqrt{(I_x - I_y)^2 + 4I_{xy}^2}}{2}. \tag{6}$$

In order to compare the deviation of the results obtained against reference results, we used two well-known error measures: the relative mean error (norm 1 – see (7)) and the relative root mean square error (norm 2 – see (8)).

$$E_1^{rel} = \frac{1}{N} \sum_{i=1}^{N} \frac{|x_i - \widehat{x}_i|}{\widehat{x}_i}, \tag{7}$$

$$E_2^{rel} = \sqrt{\frac{1}{N} \sum_{i=1}^{N} \left(\frac{|x_i - \widehat{x}_i|}{\widehat{x}_i} \right)^2}, \tag{8}$$

where x_i denotes the ith measured value (area, moment of inertia) and $\widehat{x}_i$ denotes the ith referenced value.

4   Results

In order to obtain the difference in area of interest estimation between different interpolation algorithms, we compared CT images from the group **GFilt**orig with appropriate images, by filtering level, from group **GFilt**high. The results of this comparison are shown in Figs. 6 and 7 for left and right femur respectively.

The difference in estimated area of interest obtained from interpolated images and original images filtered by level filters of 300, 400, 500, 600 and 700 HU is presented in **Table 1**.

It can be seen from the Table 1 that the difference in calculation of the cortical area from images that belong to group **GFilt**_{orig} and images from group **GFilt**_{high} is in the range 0.82 – 4.73 %, so we can say that that there is no error greater than 5% in the calculation of the cortical area from images of any group.
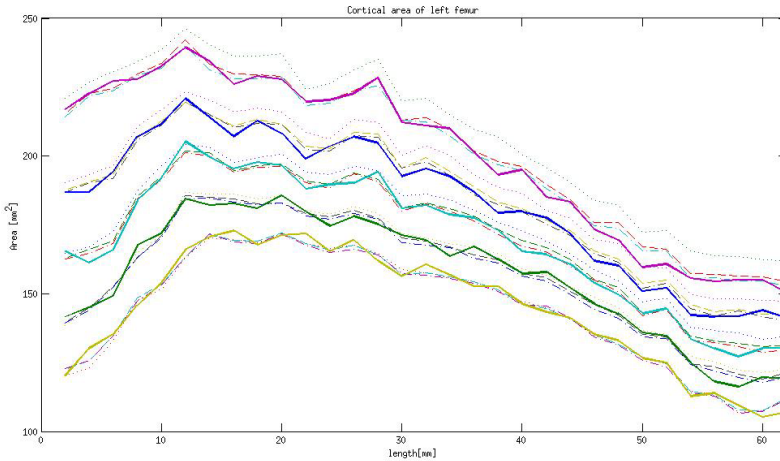
Fig. 6 – *Changing cortical cross-sectional area of the left femur along the bone length obtained by CT images from groups **GFilt**_{orig} (solid lines) and **GFilt**_{high} (dotted lines for linear, dashed lines for cubic, and dash-dot lines for spline interpolated images) passed through level filters of 300, 400, 500, 600 and 700 HU respectively (ordered top down).*
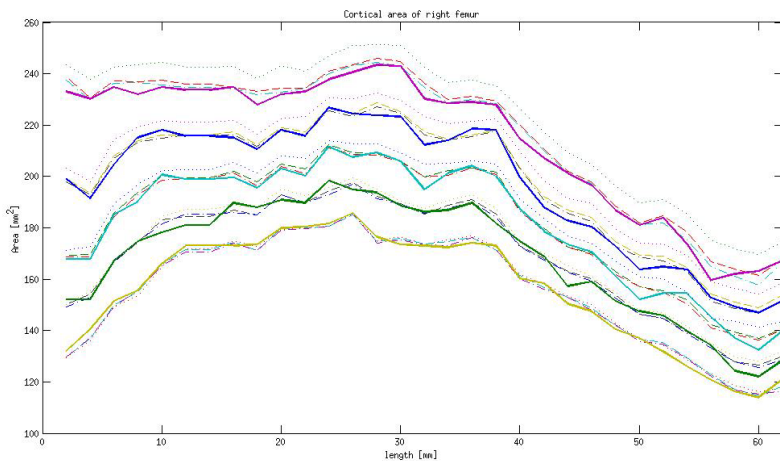
Fig. 7 – *Changing cortical cross-sectional area of the right femur along the bone length obtained by* CT *images from groups **GFilt**_{orig} (solid lines) and **GFilt**_{high} (dotted lines for linear, dashed lines for cubic, and dash-dot lines for spline interpolated images) passed through level filters of 300, 400, 500, 600 and 700 HU respectively (ordered top down).*

Table 1

Errors in area of interest obtained from CT *images*
from group **GFilt**high *against images from group* **GFilt**orig.

Error method	Inter pol.	Left femur					Right femur				
		Above 300HU	Above 400HU	Above 500HU	Above 600HU	Above 700HU	Above 300HU	Above 400HU	Above 500HU	Above 600HU	Above 700HU
E_1^{rel} [%]	Lin.	4.32	3.50	2.61	1.60	1.32	4.46	3.58	2.58	1.80	1.23
	Cub.	1.17	1.24	1.11	1.18	1.17	1.27	1.17	1.02	1.28	1.06
	Spl.	0.96	0.96	0.93	1.32	1.34	0.91	0.82	0.85	1.19	1.10
E_2^{rel} [%]	Lin.	4.73	3.74	2.95	2.09	1.76	4.65	3.83	2.96	2.36	1.48
	Cub.	1.66	1.43	1.41	1.60	1.57	1.58	1.46	1.32	1.59	1.27
	Spl.	1.30	1.12	1.14	1.53	1.66	1.28	1.09	1.24	1.51	1.35

For each CT image mentioned in Sections 2 and 3 (Material and Methods) belonging to groups **GFilt**orig and **GFilt**high, we created inner and outer contours of bone using the Canny edge detection algorithm. As can be seen from Figs. 3c and 3d, contours obtained in images with the original resolution are rough and those obtained in images with enhanced resolution are better. We used contours from images of both resolutions (i.e., **Ref**high and **Ref**orig) to calculate cross-sectional areas for comparison.

We compared cross-sectional areas of bones obtained by level filtering of CT images in the original resolution (those belonging to group **GFilt**orig) with both references. Fig. 8 shows how the calculated area changes along the bone shaft, and how the calculated area decreases with higher level filtering. The filtering levels for this experiment were: 200, 300, 400, 500, 600 and 700 HU and the results are presented using solid lines. It is evident that resulting areas of bones in images processed with higher level thresholds are lower.

From Fig. 8 demonstrates that the lines representing areas of bones calculated from images processed with level filters of 400, 500 and 600 HU are the closest lines to the **Ref**high "reference" line (presented as a dashed line in the figure) in both left and right bones.

In order to quantify the similarity (difference) between cortical areas obtained from images that belong to the group **GFilt**orig and reference images **Ref**high, we calculated the errors shown in **Table 2**.

Table 2 demonstrates that the smallest error occurs in CT images filtered by a value level of 500 HU, and the second lowest with a value of 400 HU. The largest error appears for images filtered by a value level of 600 HU.
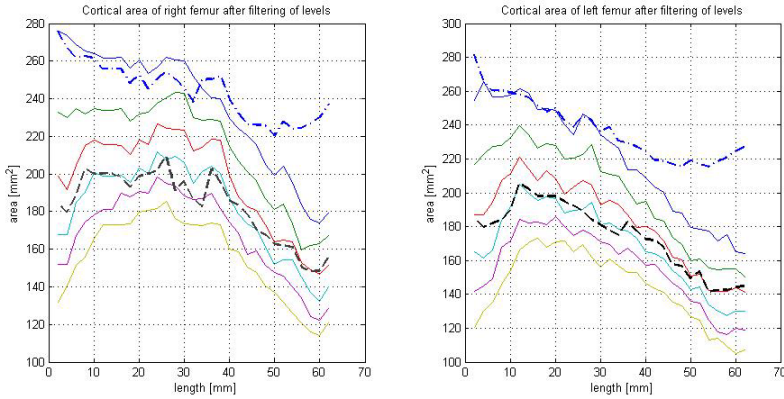
Fig. 8 – *Changing calculated cross-sectional area of femur of left and right leg along the bone length from* **GFilt**$_{orig}$ *group images passed through level filters of* 200, 300, 400, 500, 600 *and* 700 HU (*in solid lines top down*) *and referenced areas obtained by Canny edge detection of* CT *image in origina (dash dot line –* **Ref**$_{orig}$*) and higher resolution (dashed line –* **Ref**$_{high}$*).*

Table 2
Errors obtained by calculating cortical area from filtered
CT *images of group* **GFilt**$_{orig}$ *and reference images* **Ref**$_{high}$.

| Error method	Left femur			Right femur		
	Above 400 HU	Above 500 HU	Above 600 HU	Above 400 HU	Above 500 HU	Above 600 HU
E_1^{rel} [%]	7.16	4.01	8.73	4.68	4.21	10.61
E_2^{rel} [%]	8.49	5.23	10.06	5.96	5.47	11.65

In order to verify if a similar pattern existed in calculated area moments of inertia, we compared calculated polar moments of inertia from referenced images with images in original resolution that passed through level filters with thresholds of 200, 300, 400, 500, 600 and 700 HU. The results are shown in Fig. 9.

It can be seen from Fig. 9 that results of calculation of polar moments of inertia of referenced images are pretty similar to images in the original resolution, when generated by level filtering with a threshold of 500 HU.

We also calculated maximal and minimal principal moments of inertia for left and right femurs using (5) and (6); the results are shown in Fig. 10. We can see from this that the results of principal moments of inertia are also in line with other results from previous comparisons: they are similar to those obtained by level filtering with a threshold value of 500HU.
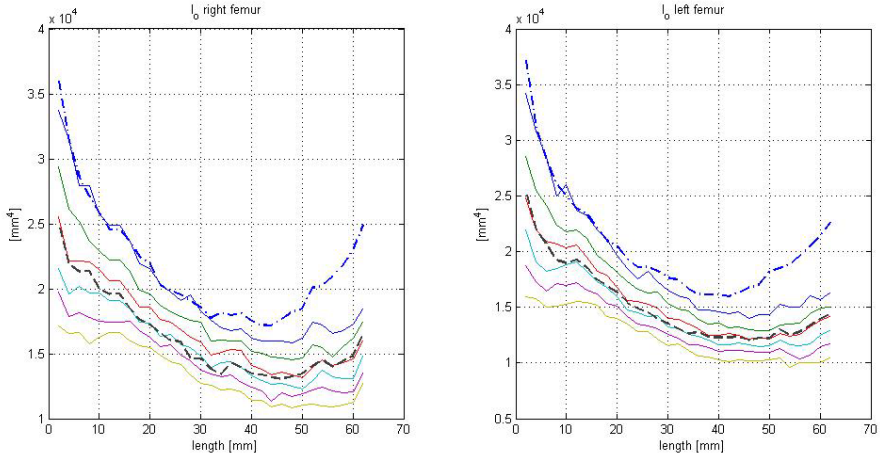
Fig. 9 – *Changing calculated polar moment of inertia of femur of left and right leg along the bone length from the images of* **GFilt**$_{orig}$ *passed through level filters of* 200, 300, 400, 500, 600 and 700 HU (*in solid lines top down respectively*) *and moments from referenced* CT *images in original* (*dash dot line –* **Ref**$_{orig}$) *and higher resolution* (*dashed line –* **Ref**$_{high}$).
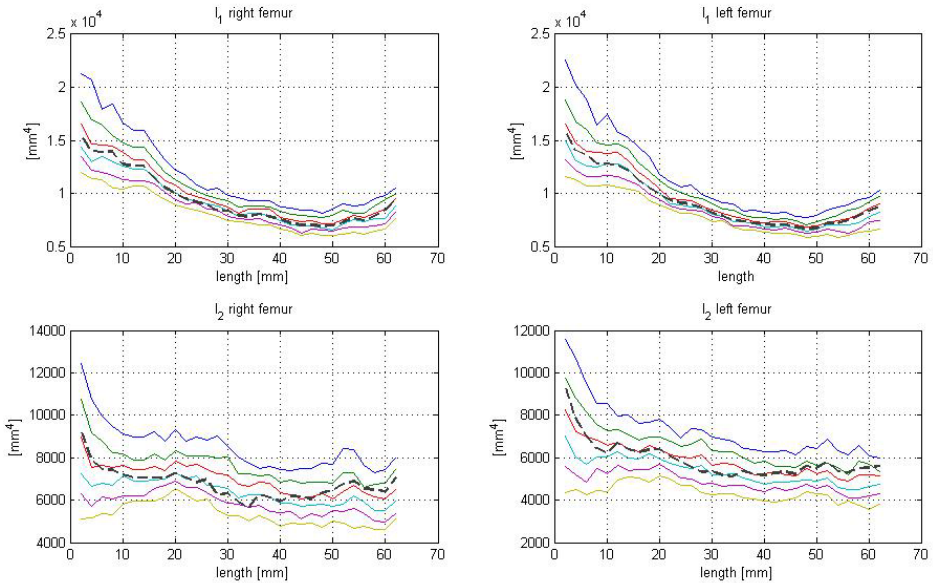
Fig. 10 – *Changing calculated principal moments of inertia of femur of left and right leg along the bone length from the images of* **GFilt**$_{orig}$ *passed through level filters of* 200, 300, 400, 500, 600 and 700 HU (*in solid lines top down respectively*) *and moments from referenced* CT *images in higher resolution* (*dashed line –* **Ref**$_{high}$).

4   Conclusion

In this paper we have described two methods to pre-process CT images of bone in order to determine relatively accurate bone cross-sectional properties. In the first method, we determined rough boundaries of bone cross-section, created an image of bone alone, and implemented filtering on image pixel values based on selected thresholds. In the second method, we increased the resolution of the bone CT image using linear interpolation, detected the inner and outer contours of bone using the Canny edge detection algorithm, and implemented a contour tracking algorithm in order to eliminate out-of contour lines. We used images obtained by the second method as reference images.

Comparison of the calculated cortical area obtained from CT images with and without increasing resolution, and filtered by level filtering, shows that there is no significant difference. However, we must point out that these results were obtained using CT images of one patient only.

By comparison of calculated cross-sectional areas and moment of inertia of the same cross-sections of bones, obtained by the methods described, we discovered that similar results for the cortical area were achieved by the first (simpler) method with a threshold of 500HU, to those created by the second (more complex) method of calculating the area from reference images, with a relative rms error of about 5%.

Our conclusion is that it is sufficient to implement the first method with a threshold level of 500HU in pre-processing of bone CT images, in order to get relatively good results for the calculation of bone geometrical cross-section properties.

6   Acknowledgement

5   References

[1]   S. Timotijević, I. Denisenko, Lj. Baščarević, R. Grbić, S. Dorović, M. Ćosić, Z. Baščarević: Biomechanical Discussion on the High Incidence of the Supracondylar Fracture of Humerus in Children, Acta Orthopedica Yugoslavica, Vol. 29, No. 1, 1998, pp. 51 – 57.

[2]   A. Web: Introduction to Biomedical Imaging, John Wiley and Sons, Hoboken, NJ, USA, 2003.

[3]   W. De Vos, J. Casselman, G.R. Swennen: Cone-beam Computerized Tomography (CBCT) Imaging of the Oral and Maxillofacial Region: A Systematic Review of the Literature, International Journal of Oral and Maxillofacial Surgery, Vol. 38, No. 6, June 2009, pp. 609 – 625.

[4] S.Z.M. Brianza, M. Delise, M.M. Ferraris, P. D'Amelio, P. Botti: Cross-sectional Geometrical Properties of Distal Radius and Ulna in Large, Medium and Toy Breed Dogs, Journal of Biomechanics, Vol. 39, No. 2, 2006, pp. 302 – 311.

[5] B.D. Snyder, D.A. Hauser-Kara, J.A. Hipp, D. Zurakowski, A.C. Hecht, M.C. Gebhardt: Predicting Fracture through Benign Skeletal Lesions with Quantitative Computed Tomography, The Journal of Bone and Joint Surgery, Vol. 88, No. 1, Jan. 2006, pp. 55 – 70.

[6] J. Rittweger, G. Beller, J. Ehrig, C. Jung, U. Koch, J. Ramolla, F. Schmidt, D. Newitt, S. Majumdar, H. Schiessl, D. Felsenberg: Bone-muscle Strength Indices for the Human Lower Leg, Bone, Vol. 27, No. 2, Aug. 2000, pp 319 – 326.

[7] H. Haapasalo, S. Kontulainen, H. Sievanen, P. Kannus, M. Jarvinen, I. Vouri, Exercise-induced Bone Gain is due to Enlargement in Bone Size without a Change in Volumetric Bone Density: A Peripheral Quantitative Computed Tomography Study of the Upper Arms of Male Tennis Players, Bone, Vol. 27, No. 3, Sept. 2000, pp. 351 – 357.

[8] C.R. Russo, F. Lauretani, S. Bandinelli, B. Bartali, A. Di Iorio, S. Volpato, J.M. Guralnik, T. Harris, L. Ferrucci: Aging Bone in Men and Women: Beyond Changes in Bone Mineral Density, Osteoporosis International, Vol. 14, No. 7, July 2003, pp. 531 – 538.

[9] E. Bobrowitsch, C. Imhauser, H. Graichen, L. Durselen: Evaluation of a 3D Object Registration Method for Analysis of Humeral Kinematics, Journal of Biomechanics Vol. 40, No. 3, 2007, pp. 511 – 518.

[10] W. Wan, P. Shi: Image Series Segmentation and Improved MC Algorithm, Journal of Shanghai Jiaotong University (Science), Vol. 13, No. 1, Feb. 2008, pp. 102 – 106.

[11] C. Mack, V. Mogallapu, A. Willis, T.P. Weldon: Exploiting Typical Clinical Imaging Constraints for 3D Outer Bone Surface Segmentation, IEEE SoutheastCon, 22 – 25 March 2007, Richmond, VA, USA, pp 519 – 523.

[12] J. Canny: A Computational Approach to Edge Detection, IEEE Transactions on Pattern Analysis and Machine Intelligence, Vol. PAMI-8, No. 6, Nov. 1986, pp. 679 – 698.

[13] J. Wu: Robust Real-time Ellipse Detection by Direct Least-square-fitting, International Conference on Computer Science and Software Engineering, Wuhan, China, 12 – 14 Dec. 2008, Vol. 1, pp. 923 – 927.

[14] D. Rašković: Otpornost materijala, Naučna knjiga, Beograd, 1987. (In Serbian)